INT. J. REMOTE SENSING, 1993, VOL. 14, NO. 11, 2231–2240

Linear mixing model applied to coarse spatial resolution data from multispectral satellite sensors

BRENT N. HOLBEN
Code 923, NASA/Goddard Space Flight Center, Greenbelt, MD, 20771, USA

YOSIO E. SHIMABUKURO
Instituto Nacional de Pesquisas Espaciais—INPE, São José dos Campos, SP, Brazil

(Received 19 April 1992; in final form 26 March 1993)

Abstract. A linear mixing model was applied to coarse spatial resolution data from the NOAA Advanced Very High Resolution Radiometer. The reflective component of the 3·55–3·95 μm channel was used with the two reflective channels 0·58–0·68 μm and 0·725–1·1 μm to run a Constrained Least Squares model to generate fraction images for an area in the west central region of Brazil. The fraction images were compared with an unsupervised classification derived from Landsat TM data acquired on the same day. In addition, the relationship between the fraction images and normalized difference vegetation index images show the potential of the unmixing techniques when using coarse spatial resolution data for global studies.

1. Introduction

Assuming the atmospheric effect is constant, the radiation detected by any sensor will be influenced by a mixture of the component surface materials (mixed pixels) unless the target is composed of a single material (pure pixel). The radiometric characteristics of the Local Area Coverage (LAC, 1·1 km pixels at nadir) of the National Oceanic and Atmospheric Administration's (NOAA) Advanced Very High Resolution Radiometer (AVHRR) are more affected by the mixed pixel problem than finer spatial resolution satellite sensor imagery.

Efforts to address the problem of mixed pixels in these data is of increasing importance as emphasis is being placed for providing global-scale monitoring (Townshend 1992). Most investigations have compared the information content of AVHRR data to fine spatial resolution data as from Landsat Thematic Mapper (TM), for example Iverson *et al.* (1989) and Cross (1990). Mixture modelling offers an alternative. Quarmby *et al.* (1992) presented a linear mixture model for crop area estimation using multi-temporal AVHRR channel 1 and 2 data. Cross *et al.* (1991) implemented a linear mixing model with the first four channels of AVHRR to monitor tropical deforestation in Rondonia, Brazil and Ghana. Two thermal infrared channels (3 and 4) were included because they were considered to contain information for forest/non-forest discrimination. This implies that each cover type is thermally distinct and the sensor response to the surface properties in question behaves linearly with thermal emission.

Thermal emission is governed by Planck's equation, therefore a linear model may not accurately represent the sensors radiometric response to a surface target. This problem may be minimized by using all reflective bands as is done with Thematic Mapper data or, as in the case of the AVHRR 3·75 μm band which is a mixture of reflected and emitted energy, use only the reflective component (Kaufman and Nakajima 1992).

Several techniques (Smith *et al.* 1985, Shimabukuro 1987, Adams *et al.* 1989) to solve the mixture problem have been applied to fine spatial resolution data sets such as Viking images of Mars (Adams *et al.* 1986); MSS (Multispectral Scanner System) and TM data (Adams and Adams 1984, Shimabukuro 1987); and AVIRIS (Airborne Visible/Infrared Imaging Spectrometer) data (Gillespie *et al.* 1990). All of the above techniques produce similar results (Shimabukuro 1987) and their use is usually dictated by an investigators personal preference.

We present a technique to apply mixture models to coarse spatial resolution AVHRR data to generate vegetation, soil, and shade fraction images from the proportion of each component within the pixels. Because of our familiarity with the method, we chose to apply the Constrained Least Squares (CLS) method (Shimabukuro and Smith 1991) to an AVHRR image covering the central-western region of Brazil. The validation of the model for this kind of data will be performed by comparing the resulting fraction images with the classification derived from coincident Landsat/TM and AVHRR NDVI images.

2. Study site

The study site is located between 17° 50′ to 18° 20′ south latitude and 52° 40′ to 53° 20′ west longitude on the border of Goias, Mato Grosso and Mato Grosso do Sul States. The site includes the Emas National Park comprising about 131 000 hectares in which the 'cerrado' vegetation is well represented (Redford 1985, IBDF/FBCN 1978). The site includes a number of small watercourses, the sources of two important rivers, riverine gallery forest and marshes, large areas of grassland (the 'campos'), and some open woodland (the 'cerrados') consisting of small thinly distributed trees seldom more than three metres high (Erize 1977). The surrounding land of the Park is used for agriculture and cattle grazing.

3. Method

3.1. *AVHRR 3·75 μm reflective component*

The AVHRR 3·75 μm band signal is a mixture of thermal and reflected energy. Typically the latter respresents less than 10 per cent of the signal for bare soil and urban features and less than 3 per cent for green vegetation (Kerber and Schutt 1986, Schutt and Holben 1991, Kaufman and Remer 1993). The reflective component may be approximated by assuming the emitted energy (brightness temperature) in the adjacent thermal band (10·5 to 11·5 μm) is related to the emitted energy in the 3·75 μm band at ambient temperature through the Planck Function as follows (Kaufman and Nakajima 1992):

$$L_3 = L_{3\rho} + L_{3\varepsilon} \quad (1)$$

where:

L_3 = Total radiant energy measured by the satellite sensor at 3·75 μm
$L_{3\rho}$ = The reflective energy at 3·75 μm
$L_{3\varepsilon}$ = The emissive ener

The reflective and emitted

where:

ρ_3 = Reflectance in the
F_o = 3·75 band solar irr
μ_o = Cosine of the solar
$R_3(T_4)$ = Emitted radia
with the Planck Function

Solving for ρ_3:

ρ_3 =

This formulation ignore
and assumes the target surf
The digital numbers are co
coefficients and Planck Fu
(Kidwell 1988).

3.2. *Linear mixture model*

The response of each
combination of the respons
Thus each image pixel con
response of each compone
model may be formulated

where:

r_i = measured satellite s
a_{ij} = spectral response o
x_j = proportion of mixt
e_i = the error term for s

Subject to:

$\Sigma x_j = 1$ and $x_j \geqslant 0$ for a

The Constrained Least
component inside the pixel
constraint is added, since
must be one and the prop
developed for three and fou
uro 1987). In this study, th
within the pixel. In additio
error image were generated

ERROR = SQRT $(r_i - \Sigma$
MEAN ERROR = $(\Sigma e_i$
where, m = number of s

$L_{3\varepsilon}$ = The emissive energy at 3·75 μm

The reflective and emitted components may be expanded according to:

$$L_3 = \rho_3 F_o \mu_o / \pi + R_3(T_4)^*(1-\rho) \tag{2}$$

where:

ρ_3 = Reflectance in the 3·75 μm band
F_o = 3·75 band solar irradiance at the bottom of the atmosphere
μ_o = Cosine of the solar zenith angle
$R_3(T_4)$ = Emitted radiance at 3·75 μm using the 11·0 μm brightness computed with the Planck Function

Solving for ρ_3:

$$\rho_3 = (L_3 - R_3(T_4))/(F_o \mu_o/\pi - R_3(T_4)) \tag{3}$$

This formulation ignores the differential atmospheric transmission in both bands and assumes the target surface is flat and the satellite sensors view direction is nadir. The digital numbers are converted to brightness temperatures using the calibration coefficients and Planck Function coefficients given in the NOAA-9 users Handbook (Kidwell 1988).

3.2. *Linear mixture model*

The response of each pixel in any spectral wavelength was taken as a linear combination of the responses of each component assumed to be in the mixed target. Thus each image pixel contains information about the proportion and the spectral response of each component within the ground resolution unit. The basic mixture model may be formulated as:

$$r_i = \Sigma a_{ij*} x_j + e_i \tag{4}$$

where:

r_i = measured satellite sensor response for a pixel in spectral band i
a_{ij} = spectral response of mixture component, j, for spectral band i
x_j = proportion of mixture component, j, for a pixel
e_i = the error term for spectral band i.

Subject to:

$\Sigma x_j = 1$ and $x_j \geqslant 0$ for all.

The Constrained Least Squares (CLS) method estimates the proportion of each component inside the pixel by minimizing the sum of squares of the errors. A linear constraint is added, since the sum of the proportions for any resolution element must be one and the proportion values must be nonnegative. This method was developed for three and four components assumed to be inside the pixel (Shimabukuro 1987). In this study, the CLS method is discussed assuming three components within the pixel. In addition, the error image for each spectral band and the mean error image were generated. They are computed for each pixel as follows:

ERROR = SQRT $(r_i - \Sigma a_{ij} x_j)2 = e_i$, and
MEAN ERROR = $(\Sigma e_i)/m$
where, m = number of spectral bands.

3.3. *Approach*

The CLS method was applied using TM and AVHRR data acquired on 29 July 1988. The imagery, centred on Emas National Park, covers approximately 100 by 100 km and 560 by 560 km for TM and AVHRR respectively. For this study, only TM channels 3 (0·63–0·69 μm), 4 (0·76–0·90 μm), and 5 (1·55–1·75 μm) were available. The AVHRR, channels used were 1 (0·58–0·68 μm), 2 (0·725–1·1 μm), and the reflective component of channel 3 (3·55–3·93 μm).

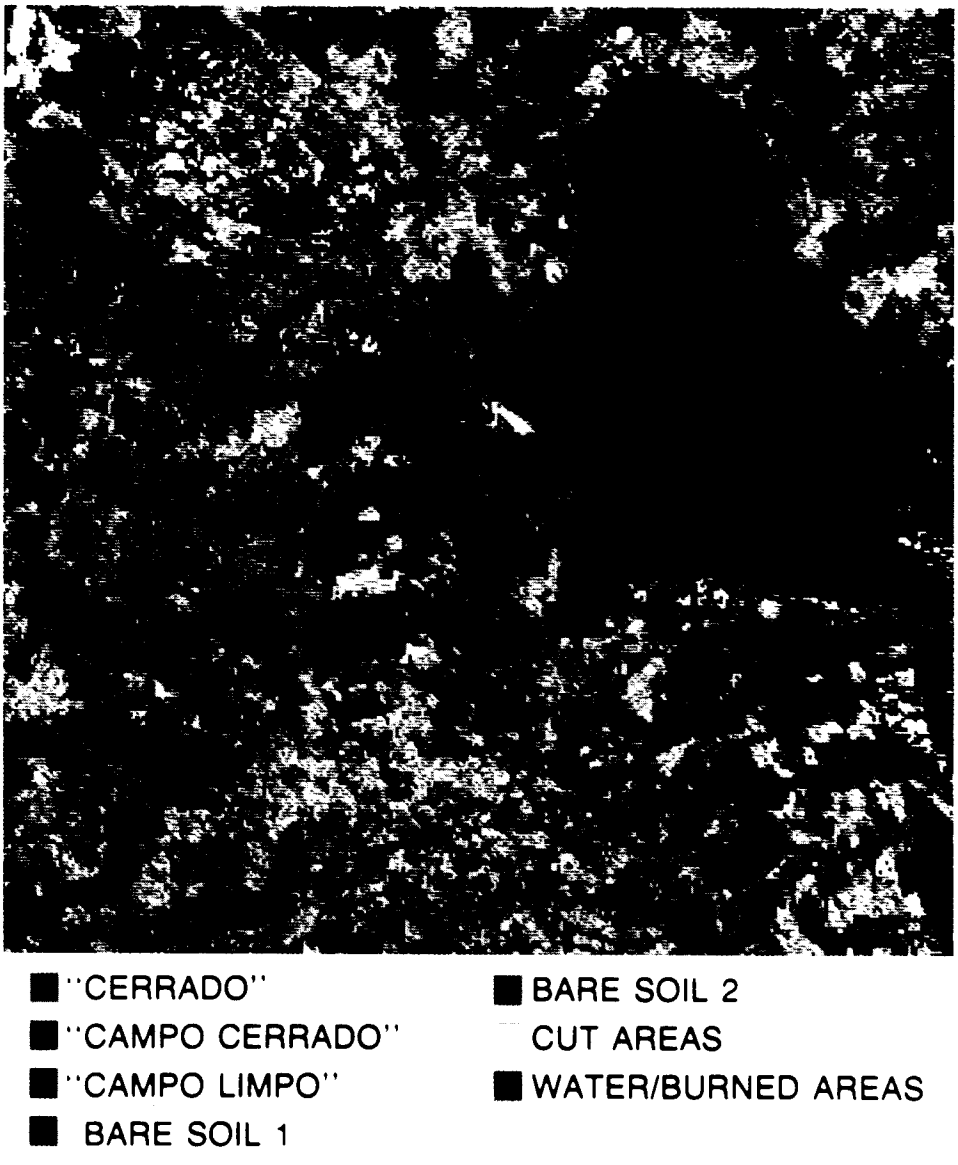

Figure 1. Land cover classification derived from Landsat TM data using unsupervised classification (K-means).

Table 1. Spectral responses
re

Channel	r^2
1	0·78
2	0·93
3Refl	0·78

n = 50

The 'pure pixel' for ea
the image. The spectral r
estimated by regressing e
the TM fraction images
derived from the regressio
derived fraction images w
difference vegetation inde

Figure 2. Colour composite

3.3. *Approach*

The CLS method was applied using TM and AVHRR data acquired on 29 July 1988. The imagery, centred on Emas National Park, covers approximately 100 by 100 km and 560 by 560 km for TM and AVHRR respectively. For this study, only TM channels 3 (0·63–0·69 μm), 4 (0·76–0·90 μm), and 5 (1·55–1·75 μm) were available. The AVHRR, channels used were 1 (0·58–0·68 μm), 2 (0·725–1·1 μm), and the reflective component of channel 3 (3·55–3·93 μm).

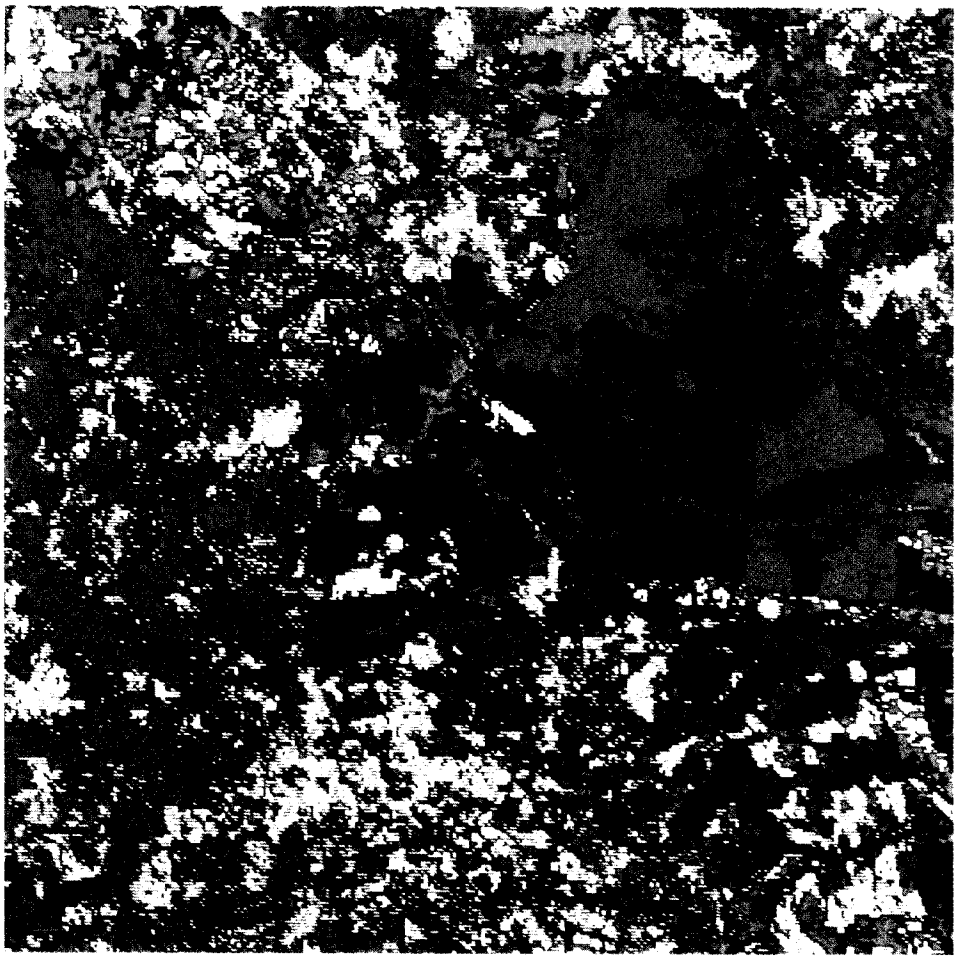

Figure 1. Land cover classification derived from Landsat TM data using unsupervised classification (K-means).

Table 1. Spectral responses re

Channel	r^2
1	0·78
2	0·93
3Refl	0·78

n = 50

The 'pure pixel' for ea the image. The spectral r estimated by regressing e the TM fraction images derived from the regressi derived fraction images w difference vegetation inde

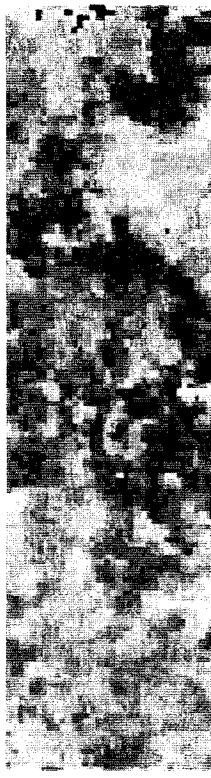

Figure 2. Colour composite

Table 1. Spectral responses for vegetation, soil, and shade for AVHRR channels estimated regressing with the TM fraction images.

Channel	r^2	DN Vegetation	DN Soil	DN Shade
1	0·781	21·8	27·8	11·3
2	0·933	46·5	42·2	10·3
3Refl	0·782	5·9	8·4	0·0

n = 50

The 'pure pixel' for each mixture component in the TM scene was selected from the image. The spectral responses for vegetation, soil, and shade for AVHRR were estimated by regressing each AVHRR channel against the corresponding pixels in the TM fraction images (Richardson *et al.* 1975). The spectral responses were derived from the regression coefficients and used as inputs for the CLS model. The derived fraction images were compared to the TM results, and related to normalized difference vegetation index NDVI images for model validation.

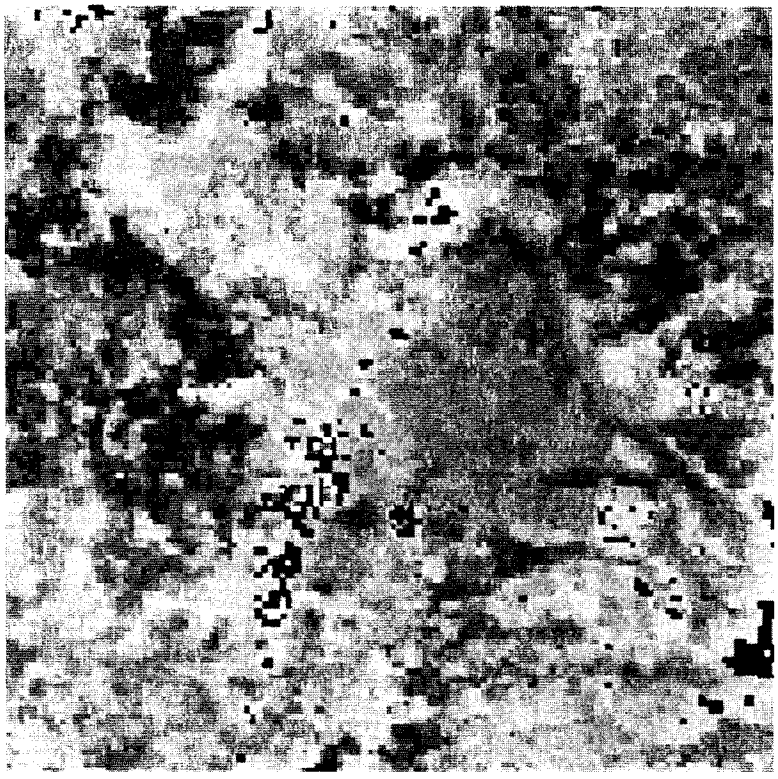

Figure 2. Colour composite of fraction image (vegetation = red, soil = green, and shade = blue) derived from AVHRR data.

Table 1. Spectral responses for vegetation, soil, and shade for AVHRR channels estimated regressing with the TM fraction images.

Channel	r^2	Vegetation	DN Soil	Shade
1	0·781	21·8	27·8	11·3
2	0·933	46·5	42·2	10·3
3Refl	0·782	5·9	8·4	0·0

n = 50

The 'pure pixel' for each mixture component in the TM scene was selected from the image. The spectral responses for vegetation, soil, and shade for AVHRR were estimated by regressing each AVHRR channel against the corresponding pixels in the TM fraction images (Richardson *et al.* 1975). The spectral responses were derived from the regression coefficients and used as inputs for the CLS model. The derived fraction images were compared to the TM results, and related to normalized difference vegetation index NDVI images for model validation.

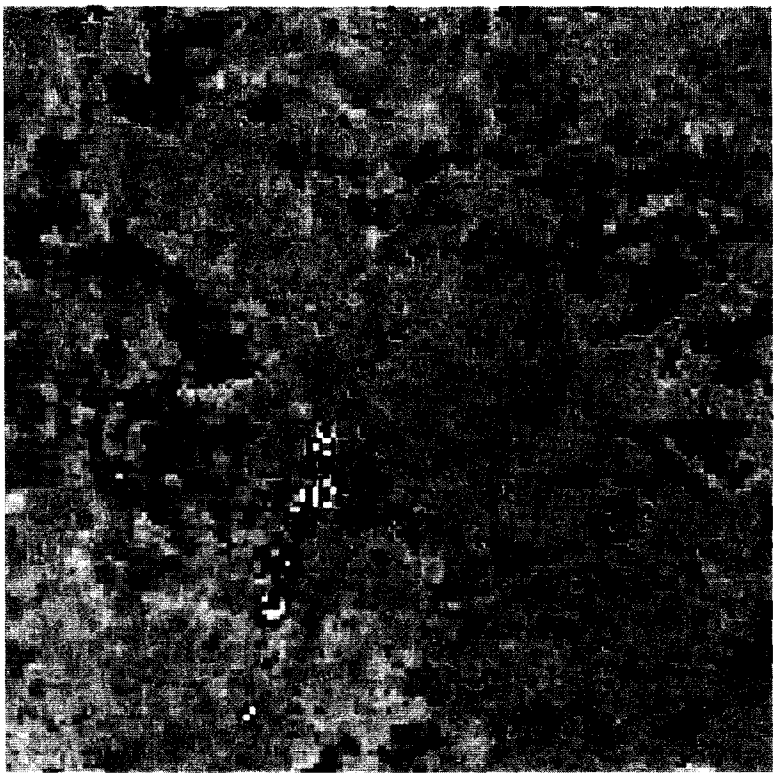

Figure 2. Colour composite of fraction image (vegetation = red, soil = green, and shade = blue) derived from AVHRR data.

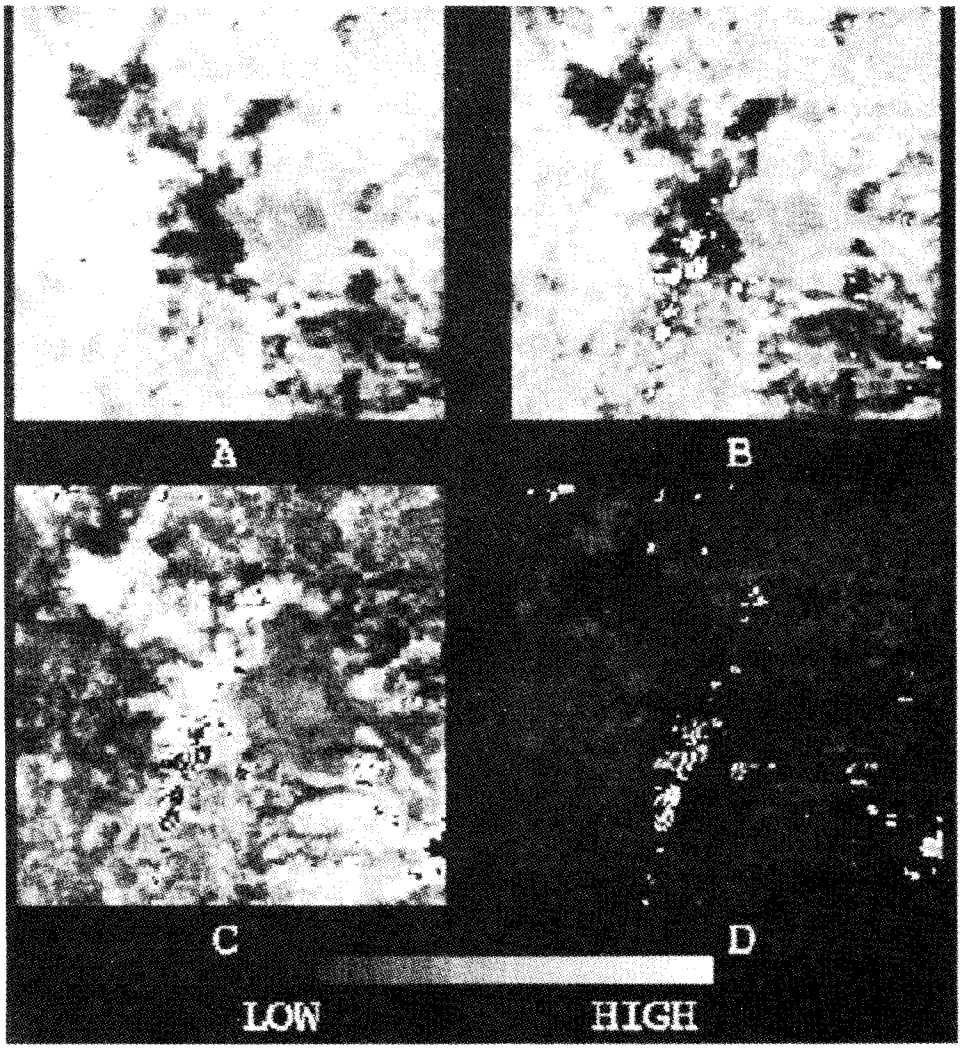

Figure 3. (A) NDVI, (B) vegetation, (C) soil and (D) mean error images derived from AVHRR data over the study site.

4. Results and discussion

The unsupervised classifier, based on K-means, identified 13 clusters and were rearranged into the following 7 classes according to ground truth reported by Shimabukuro *et al.* (1991): Water and burned areas, 'cerrado', 'campo cerrado', 'campo limpo', bare soil 1, bare soil 2, and cut areas (figure 1). The spectral response for shade was searched in water and burned areas classes based on similar low spectral responses (Richardson *et al.* 1975, Adams *et al.* 1986, Shimabukuro 1987, Gillespie *et al.* 1990). The spectral responses for vegetation and soil were searched inside the 'cerrado' and cut areas classes, respectively.

The coefficient of determination, r^2, and the spectral responses of the components for the AVHRR channels are presented in table 1. The vegetation, soil, and shade fraction images were
model for AVHRR data (fi
1), in general, there is a
fraction images is that th
component within the pixe
and shade = blue), yellow
bare soil.

There was a visual simil
and B). The NDVI values w
0·900 for TM (n = 75) an
agreement between the hi
clusters from the unsuperv
performed on these data se
mean error images (figure
aggregates.

Figure 4. Vegetation fractio

shade fraction images were generated using these spectral responses in the mixture model for AVHRR data (figure 2). Comparing to the TM classification result (figure 1), in general, there is a good agreement between them. The advantage of the fraction images is that they contain physical information, i.e., amount of each component within the pixel. For example, in figure 2 (vegetation = red, soil = green, and shade = blue), yellow means that a pixel has some amount of vegetation and bare soil.

There was a visual similarity of vegetation fraction and NDVI images (figure 3A and B). The NDVI values were well correlated by the fraction images ($r^2 = 0{\cdot}952$ and 0·900 for TM (n = 75) and AVHRR (n = 90), respectively). Also there is good agreement between the higher soil pixel values and the corresponding bare soil clusters from the unsupervised classification. Note that cloud screening was not performed on these data sets yet they are easily detected in the vegetation, soil and mean error images (figure 3B, C, and D) as a vertical line of light coloured cell aggregates.

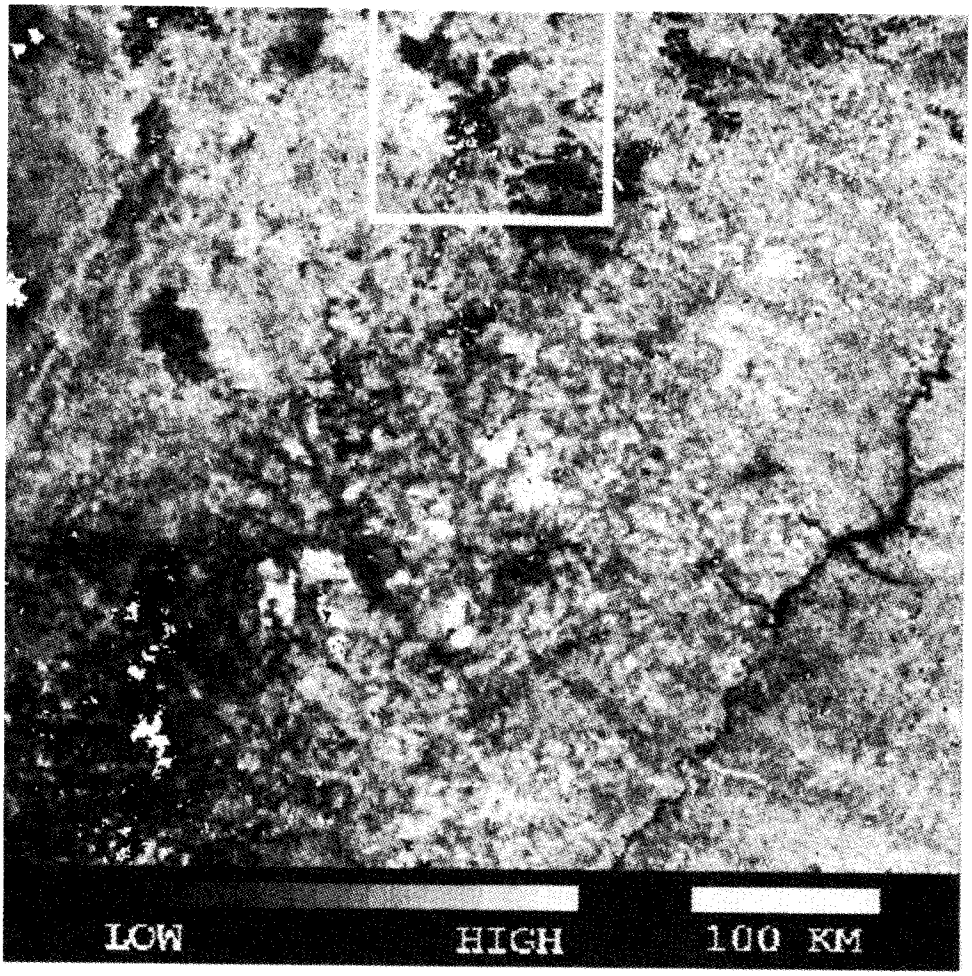

Figure 4. Vegetation fraction image derived from AVHRR data covering a large area around the study site.

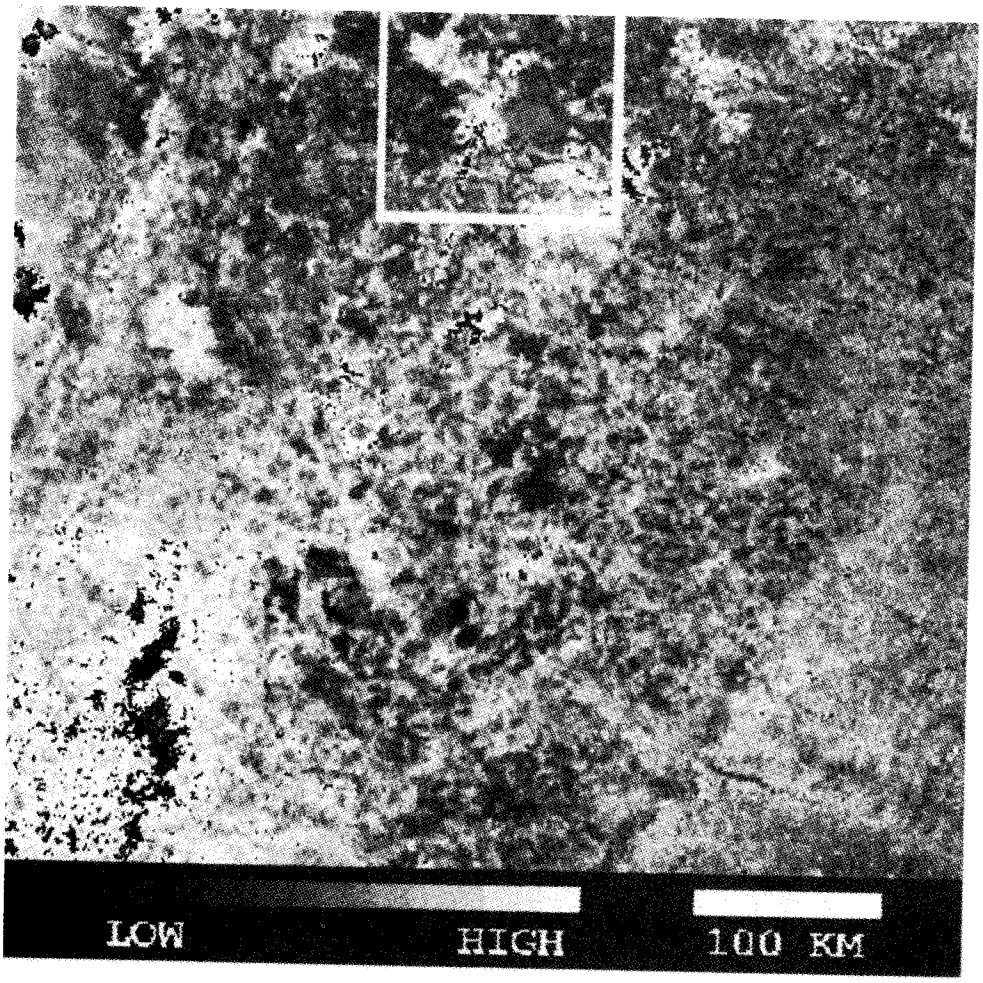

Figure 5. Soil fraction image derived from AVHRR data covering a large area around the study site.

Figures 4 and 5 show the vegetation and soil fraction images, respectively, derived from AVHRR data over a large area (512 by 512 pixels) around the study site. Again the similarity between NDVI and vegetation fraction shows the potential of extending the linear mixture technique well beyond the boundaries of the defining components using coarse spatial resolution data. As stated previously, the disagreement between these images for the cloudy pixels indicates a cloud screening algorithm must be employed for most large area investigations. In addition, the soil fraction image seems to be useful for tropical deforestation studies since it contains information about bare soil proportion within the pixels. Also, the shade image contains information that can explain the vegetation index response, especially for the tropical forest which from the multi-layer structure has a high amount of shade.

5. Conclusions

As the information contained in the AVHRR remote sensing resolution elements are mostly a mixture of several components, the linear mixing models appear to be a useful tool for image ana
tions is required to ful
evaluation of the techniqu
apply the approach to co

Acknowledgment

We wish to thank Kas
at the Global Inventory
thanks to John Schutt and
the 3·75 μm band. Durin
serving as a Visiting Scie
auspices of the Universiti

References

ADAMS, J. B., and ADAMS, J. I
removing vegetation b
Conference on Remote
(Michigan: ERIM), pp
ADAMS, J. B., SMITH, M. O.,
analysis of rock and
Research, **91**, 8098–81
ADAMS, J. B., SMITH, M. O.,
surfaces: a strategy fo
International Geoscienc
Symposium on Remote
CROSS, A. M., 1990, AVHR
Proceedings of the In
(IGARSS'90), Washin
CROSS, A. M., SETTLE, J. J
measurement of tropic
Remote Sensing, **12**, 1
ERIZE, F., 1977, Brazil's fines
GILLESPIE, A. R., SMITH, M. O
D. E., 1990, Interpreta
images, Owens Valley
AVIRIS, JPL, Pasaden
IBDF/FBCN (Instituto Brasi
Conservacao da Natu
(Brasilia: IBDF/FBCN
IVERSON, L. R., COOK, E. A.,
validating forest cover
International Journal of
KAUFMAN, Y. J., and NAKAJI
and albedo. Submitted
KAUFMAN, Y. J., and REMER,
channel, (in preparatio
KERBER, J. A., and SCHUTT, J.
Mapping. *Photogramm*
KIDWELL, K. B., 1988, NOAA
NOAA-9, NOAA-10 a
and Atmospheric Admi
QUARMBY, N. A., TOWNSHEND
T. L., and SILLEOS, N.,
crop estimation. *Interna*

useful tool for image analysis. Further quantitative assessment of the pixel proportions is required to fully interpret the results from mixture models. Rigorous evaluation of the technique beyond the region of component definition is required to apply the approach to coarse resolution data such as AVHRR.

Acknowledgment

We wish to thank Kashka Donaldson and Wayne Newcomb for their assistance at the Global Inventory Mapping and Monitoring (GIMMS) Laboratory. Our thanks to John Schutt and Yoram Kaufman for their useful conversations regarding the 3·75 μm band. During the preparation of this manuscript, the Co-author was serving as a Visiting Scientist at NASA Goddard Space Flight Center under the auspices of the Universities Space Research Association (USRA).

References

ADAMS, J. B., and ADAMS, J. D., 1984, Geologic mapping using Landsat MSS and TM images: removing vegetation by modeling spectral mixtures. *Proceedings of the Third Thematic Conference on Remote Sensing for Experimental Geology, Colorado Springs, Colorado*, (Michigan: ERIM), pp. 615 622.

ADAMS, J. B., SMITH, M. O., and JOHNSON, P. E., 1986, Spectral mixture modeling: a new analysis of rock and soil types at the Viking Lander 1 site. *Journal of Geophysical Research*, **91,** 8098 8112.

ADAMS, J. B., SMITH, M. O., and GILLESPIE, A. R., 1989, Simple models for complex natural surfaces: a strategy for the hyperspectral era of remote sensing. *Proceedings of the International Geoscience and Remote Sensing Symposium (IGARSS'89)/12th Canadian Symposium on Remote Sensing, Vancouver, Canada*, (New York: I.E.E.E.), pp. 16–21.

CROSS, A. M., 1990, AVHRR as a data source for a GIS: deforestation in Amazonia. *Proceedings of the International Geoscience and Remote Sensing Symposium 1990 (IGARSS'90), Washington, D.C.*, (New York: I.E.E.E.), pp. 223–226.

CROSS, A. M., SETTLE, J. J., DRAKE, N. A., and PAIVINEN, R. T. M., 1991, Subpixel measurement of tropical forest cover using AVHRR data. *International Journal of Remote Sensing*, **12,** 1119 1129.

ERIZE, F., 1977, Brazil's finest National Park. *Oryx*, **13,** 457–462.

GILLESPIE, A. R., SMITH, M. O., ADAMS, J. B., WILLIS, S. C., FISCHER, A. F. III, and SABOL, D. E., 1990, Interpretation of residuals images: spectral mixture analysis of AVIRIS images, Owens Valley, California. *Proceedings of the Airborne Science Workshop: AVIRIS, JPL, Pasadena, CA*, (JPL Publication 90-54), pp. 243–270.

IBDF/FBCN (Instituto Brasileiro de Desenvolvimento Florestal/Fundacao Brasileira para Conservacao da Natureza), 1978, *Plano de Manejo—Parque Nacional de Emas*. (Brasilia: IBDF/FBCN).

IVERSON, L. R., COOK, E. A., and GRAHAM, R. L., 1989, A technique for extrapolating and validating forest cover across large regions: Calibrating AVHRR data with TM data. *International Journal of Remote Sensing*, **10,** 1805–1812.

KAUFMAN, Y. J., and NAKAJIMA, T., 1992, Effect of Amazon smoke on cloud microphysics and albedo. Submitted to *Journal of Applied Meteorology*, Squires Special Issue.

KAUFMAN, Y. J., and REMER, L., 1993, Remote sensing of vegetation in the mid-IR: the 3·75 channel, (in preparation).

KERBER, J. A., and SCHUTT, J. B., 1986, Utility of AVHRR Channels 3 and 4 in Land-Cover Mapping. *Photogrammetric Engineering and Remote Sensing*, **52,** 1877–1883.

KIDWELL, K. B., 1988, NOAA polar orbiter data (TIROS-N, NOAA-6, NOAA-7, NOAA-8, NOAA-9, NOAA-10 and NOAA-11) users guide. (Washington, D.C. 20233: Oceanic and Atmospheric Administration).

QUARMBY, N. A., TOWNSHEND, J. R. G., SETTLE, J. J., WHITE, K. H., MILNES, M., HINDLE, T. L., and SILLEOS, N., 1992, Linear mixture modelling applied to AVHRR data for crop estimation. *International Journal of Remote Sensing*, **13,** 415–425.

REDFORD, K. H., 1985, Emas National Park and the plight of the Brazilian cerrados. *Oryx*, **29,** 210–214.

RICHARDSON, A. J., WIEGAND, C. L., GAUSMAN, H.W., CUELLAR, J. A., and GERBERMANN, A. H., 1975, Plant, soil and shadow reflectance components of row crops. *Photogrammetric Engineering and Remote Sensing*, **41,** 1401–1407.

SCHUTT, J. B., and HOLBEN, B. N., 1991, Estimation of Emittances and Surface Temperatures from AVHRR data. *Proceedings of the International Geoscience and Remote Sensing Symposium 1991 (IGARSS'91), Espoo, Finland*, (New York: I.E.E.E.), pp. 1179–1181.

SHIMABUKURO, Y. E., 1987, Shade images derived from linear mixing models of multispectral measurements of forested areas. Ph.D. Dissertation, Colorado State University, Fort Collins, CO.

SHIMABUKURO, Y. E., and SMITH, J. A., 1991, The least-squares mixing models to generate fraction images derived from remote sensing multispectral data. *I.E.E.E. Transactions on Geoscience and Remote Sensing*, **GE-29**, 16–20.

SHIMABUKURO, Y. E., SANTOS, J. R., LEE, D. C. L., and PEREIRA, M. C., 1991, Remote sensing data for monitoring and evaluating burned areas: case of Emas National Park (GO). *Pesquisa Agropecuaria Brasileira*, **26,** 1589–1598.

SMITH, M. O., JOHNSON, P. E., and ADAMS, J. B., 1985, Quantitative determination of mineral types and abundances from reflectance spectra using principal component analysis. *Journal of Geophysical Research*, **90,** 792–804.

TOWNSHEND, J. R. G., 1992, Improved Global Data for Land Applications, A proposal for a new High Resolution Data Set. IGBP, Global Change, Report No. 20, The International Geosphere-Bioshpere Programme: A Study of Global Change (IGBP) of the International Council of Scientific Unions (ICSU) Stockholm, 87p.